

Deformation mechanism and optimum design for large cross-sectional longwall installation roadway under compound roof

H.C. Zhao^{1 and 2*}, H.J. An³ and M.S. Gao^{1 and 3}

1. School of geology and mining engineering, Xinjiang University, Urumqi, Xinjiang, China

2. School of Civil, Mining and Environmental Engineering, University of Wollongong, Wollongong, NSW, Australia

3. School of Mines, China University of Mining and Technology, Xuzhou, Jiangsu, China

Received 5 October 2017; received in revised form 17 July 2018; accepted 6 August 2018

*Corresponding author: hz449@uowmail.edu.au (H.C. Zhao).

Abstract

Both the deformation characters and the failure mode of the large cross-sectional longwall installation roadway under compound roof are becoming an emergent issue than ever before due to the rapid development of modern mining equipment. Various engineering applications have revealed that the insufficient design and inappropriate support technology are the main reasons for the fatal accidents associated with the sudden roof fall attributed to the separation of the overlying compound strata. The present research work, therefore, starts with a case study using the conventional support technology in order to demonstrate the importance of this issue followed by a summarization of the typical failure mode of the longwall installation roadway under compound strata with varied thicknesses. Then a simplified theoretical model is proposed and set up aiming at a better understanding of the distribution of the elastic-plastic zones as well as the effects of different caving procedures. The finite element analysis software program FLAC3D is adopted to evaluate the effect of the caving method and the reinforcement provided by an additional support. Then a case study conducted at a typical coal mine with compound roof condition is presented to verify the advantages of the proposed design. The results obtained show that the optimized design presented in this research work is effective to control the deformation of the surrounding rock, particularly in terms of separation of the overlying compound strata.

Keywords: *Longwall Mining, Installation Roadway, Compound Roof, Large Cross-Section, Theoretical Analysis.*

1. Introduction

With the rapidly increasing demand of black coal in the recent years, a large amount of mining equipment with a large scale cross-section including coal shearer and self-advancing hydraulic support are being widely used in more and more modern coal mines, resulting in an unpreventable increase in the cross-section of either the tailgate/main gate or the installation roadway for longwall working face. Compared to the traditional roadway with a normal size, for which the combined support technology can be successfully used to maintain the stability of the surrounding rock, the insufficient design and inappropriate support technology are the main

reasons for the fatal accidents associated with the sudden roof fall attributed to the separation of the overlying compound strata for this kind of longwall installation roadway. Moreover, this situation is more complex for compound roof consisting of different soft layers and/or hard coal gangue.

During the past two decades, various investigations, either in terms of the theoretical analysis or the field application, have been carried out to better understand the deformation mechanics of the roadway under the compound roof with different geological conditions. These observations have revealed the effect of

compound roof on the stability of the surrounding rocks, resulting in the occurrence of several useful support technologies, which have been verified by successful practical applications. Jiang et al. [1] have carried out a theoretical study to set up the classification index associated with the cable status. Based on this classification, an assessment system has been proposed and verified by practical applications. Manchao et al. [2] have investigated the deformation and damage mechanisms of a roadway with compound roof in deep mining, revealing that the non-linear mechanisms of the surrounding rocks are an important issue for controlling the stability of the roadway. Xiao et al. [3] have introduced the application of full-length bonded high-strength bolts combined with a highly strong pre-stressed cable to control the stability of a roadway in an extremely soft coal seam with compound roof. Chengwen et al. [4] and Zhang et al. [5] have presented the case study of a roadway with a complex roof condition, the result of which indicated that the quality control was the other main concern for the stability of the surrounding rocks. Frith et al. [6] have discussed the effect of layered roof strata on the stability of the surrounding rocks to find out the fundamental principles of an effective reinforcing roof bolting strategy. These aforementioned investigations do mainly focus on the stability of a roadway with compound roof, the cross-section of which is of normal size.

With an increase in the cross-sectional size, the control of the surrounding rocks is believed to be more critical, exemplified by the installation roadway with a large scale cross-section. The longwall installation roadway is normally excavated by “two-pass” installation from the boundary of the mining area to form the working face. The long trends can be used for the first pass, and then some other conventional supports such as bolts and cables can be applied to restrict the movement of the overlying strata. The problem is that the de-bonding of the installed primary supports is caused by the unpredicted movement of the upper stratum. Colwell et al. [7] have summarized the current practices and outcomes of the longwall installation roadway and introduced the design methodology termed as the analysis and design of face-road roof support (ADFRS) for mining engineers to maintain the stability of the longwall installation roadway. Seedsman et al. [8] have presented a case study of the application of a pre-installed cable in longwall installation roadways, from which it is apparent

that the conventional cable cannot prevent the onset or progression of failure owing to its high stiffness. Bai et al. [9, 10] have presented the failure mode of the longwall installation roadway with a large span under a water-rich roof by numerical investigations. It has been well-understood that the influence of increasing the cross-sectional size of the roadway is the key parameter for coal mine operators to maintain the stability of the surrounding rocks. The weak roof is becoming a critical issue for roof control for coal mines, as discussed by Payne [11]. Even though to the best of our knowledge no systematic analysis was carried out to analyze the failure mode of the large scale cross-sectional longwall installation roadway with compound roof, there should be another research topic for both the coal operators and the scholars. As a result, both the deformation characteristics and the selection of the key support parameters are desirable to be well-investigated.

Against this background, the present research work starts with a summarization of the deformation characteristics of the longwall installation roadway with a large cross-sectional size based on a typical failure case study conducted at the Chenjiazhuang coal mine. Based upon the natural equilibrium arch theory, the simplified analysis model was proposed in order to evaluate the sensitive parameters followed by the field investigation using the corresponding support technology to verify the advantages of the mentioned optimal design.

2. Geological condition and failure mode of longwall installation roadway

The longwall installation roadway in the No.90103 working panel with a large scale cross-sectional size is the first trail for the Chenjiazhuang coal mine with a mining depth of 500-545 m. The Chenjiazhuang coal mine located at the Shan-xi Province, NW China, is a modern coal mine with a production capacity of 0.9 Mt/a (Figure 1). The width and height of the longwall installation roadway are 8 m and 3.7 m, respectively. The average thickness of the mining coal seam (9#) is 1.15 m with an inclination of 7~12°. It is apparent from the stratigraphic column (Figure 1) that the immediate roof consists of 9 different typical strata, the thickness of which ranges from 0.40 m to 0.85 m. On top of these overlying strata, the key basic roof consisting of siltstone is observed with a thickness of 6.30 m. According to the definition of compound roof, as mentioned earlier, the geological condition of the

installation roadway in the No.90103 working panel belongs to a typical target with compound roof.

The longwall installation roadway began with the $\phi 20 \times 2200$ mm highly strong bolts installed as a primary support with an inter row spacing of 800×800 mm. In addition, two additional cables, the diameter and length of which were 15.24 mm and 7300 mm, respectively, were installed between two rows of bolt as a secondary support. A more detailed information can be seen in Figure 2. However, it is not a long time since the presented support technologies were applied and the fatal roof fall occurred, as shown in Figure 3.

The main reasons for the failure of the intallation roadway can be summrarized as follow: 1) The poor quality control attributed to the enlarged cross-section of the roadway than that designed. The widest width of the roadway was nearly 9.0 m at some sites. A much larger span of the roadway leads to a premature failure of the compound roof 2) The insufficienet desgin of the priminary support is belived to be another important issue for the unexpected failure. The relavtely low strength of the support in two ribs associated with the slip caused the enlarged cross-section as well 3) The low pre-stress applied on the bolt is an unacceptable issue for the support. Even though it should be prevented in pratical applications, it has

still been observed in the longwall installalton roadway, as shown in Figure 3, indicating that the bolt was not well-installed according to the standard.

The typical failure modes of the large scale cross-sectiononal longwall installation roadway under compound roof are presnted in Figure 4. It can be divided into two different categories according to the deformation characters of the overlying stratua. As shown in Figure 4a, the obvious de-bonding is easy to form owing to the different tensile strength of the ovelying strata termed as Roof #1, 2, and 3 with varied thicknesses. The overlying strata nearby the roof surface are seriously affected because the tensile strength is normally lower than that of the compressive stregnth for the surrounding rocks. In addition, the movement of two ribs may also lead to an increase in the span of roadway, which will accelerate the damage of the roof. Figure 4b presents another type of failure mode associated with the seperation of compound roof due to an insufficient support strength, as pointed out earlier. For this situation, a sudden roof fall will occur, although the continious deformation is not observed before the occurance of the roof fall. The latter failure mode is belived to be more dangerous than that of the first one since it emerges suddenly without any obvious symptom.

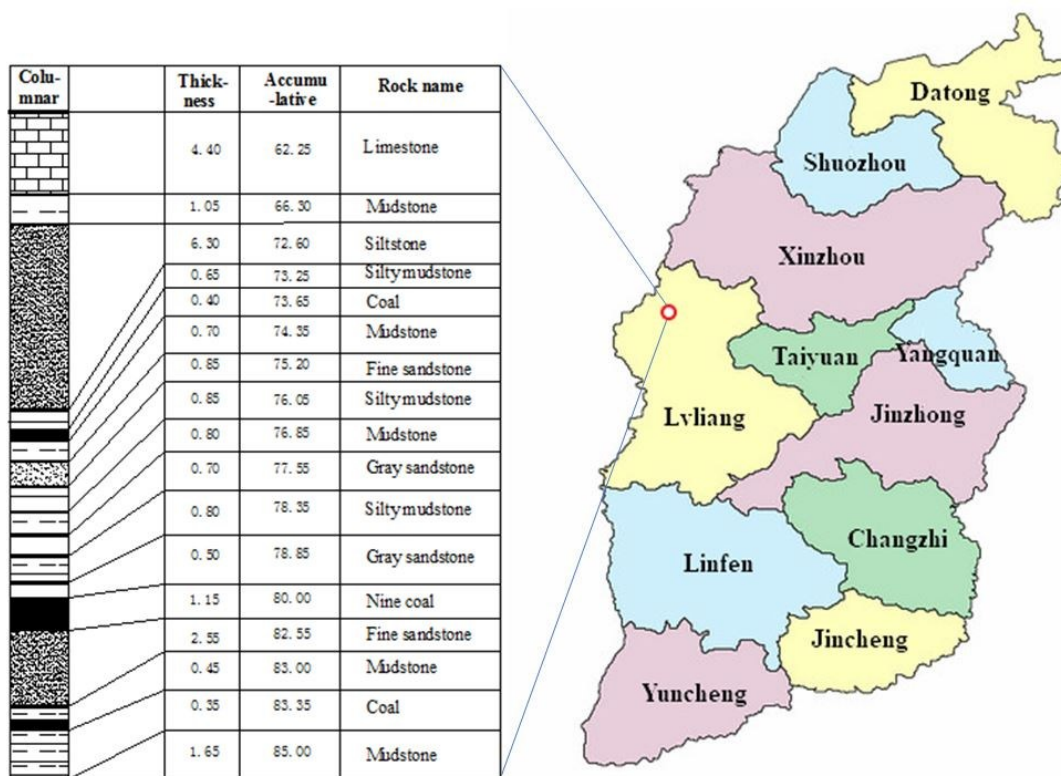


Figure 1. Stratigraphic column of roof geology and location of the coal mine.

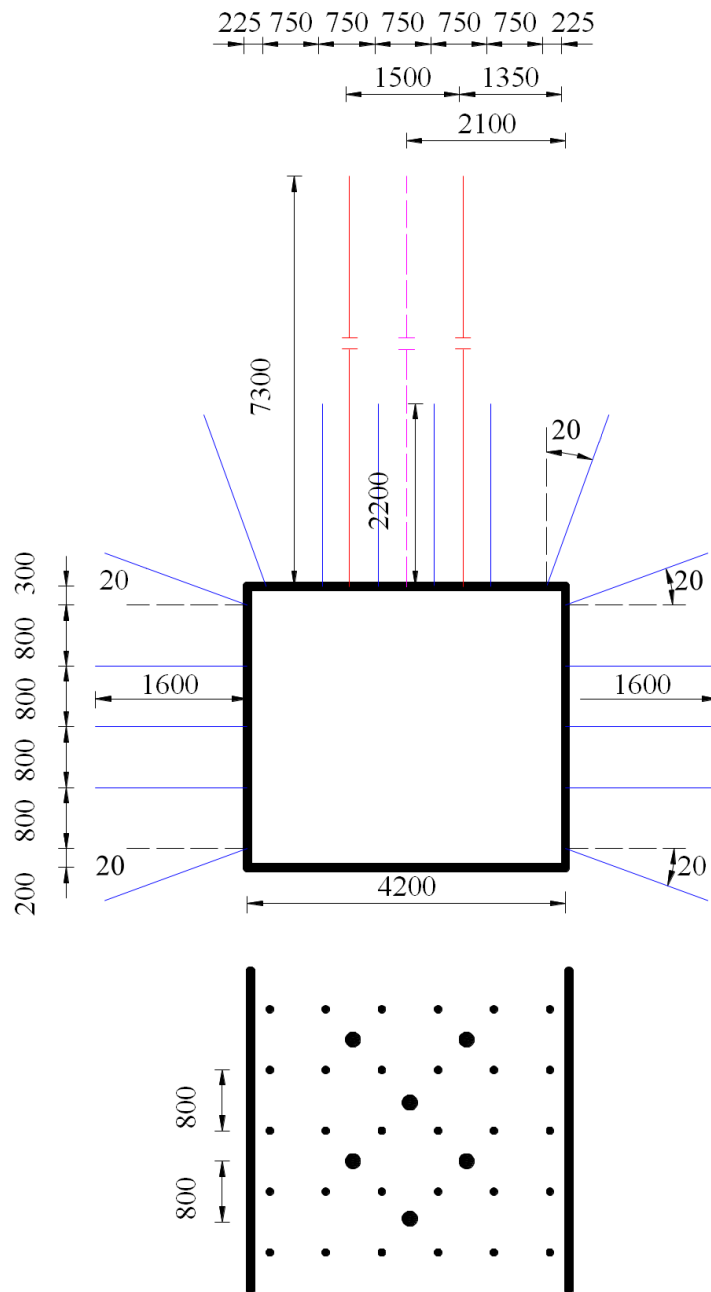


Figure 2. Primary support and reinforced sketch for longwall installation roadway.



Figure 3. Failure mode of longwall installation roadway.

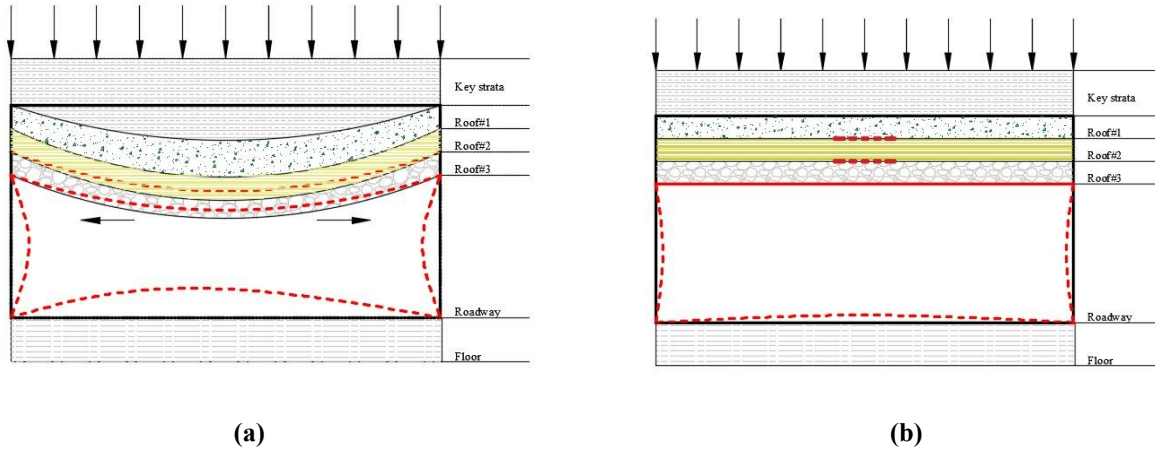


Figure 4. Typical failure modes of large cross-sectional roadway under compound roof.

3. Theoretical analysis model

3.1. Revised natural equilibrium arch theory

For the longwall installation roadway under compound roof, the roof deformation is believed to be the main concern, even though both the ribs and floor are also affected by the compound stratum. Therefore, the theoretical analysis model termed as the revised natural equilibrium arch theory [12-15] is introduced to evaluate the deformation mechanism of the longwall installation roadway.

The basic assumption of the revised natural equilibrium arch theory is that the deformation mechanism of the overlying strata can be simplified to natural equilibrium. This has been successfully verified by several practical applications, where the artificial support cannot provide a sufficient load carrying capacity for deep mining without the existing natural equilibrium. Since the revised model is developed on the basis of the natural equilibrium theory, the revised theory can also meet the basic assumptions of the natural equilibrium. The readers may refer to Miao (1990) [15] for more details of the model.

As shown in Figure 5, the oval natural equilibrium arch is normally formulated under the combinational effects of the vertical pressure (i.e. q) and the horizontal pressure (i.e. λq). Herein, λ is the ratio of horizontal pressure and vertical pressure. For ease of reference, different symbols are used in the present work: a represents the half width of the roadway; a_2 is denoted as the radius of the arch; b_1 is the height of the arch on the top

surface of roadway; b_2 is the height of the arch; l is equal to $b_2 - b_1$; and θ is used to represent the collapse angle of the arch.

There is no shear stress and moment on the cross-section of the arch, and therefore, the equilibrium arch apsidal equation can be obtained by calculation of the moment for point M from point A [15]:

$$\frac{x^2}{a_2^2} + \frac{(y+l)^2}{b_2^2} = 1 \quad (1)$$

where $a_2^2 = \lambda b_2^2$ and $b_1 = b_2 - l$.

that is:

$$x^2 + \lambda(y+l)^2 = a_2^2 \quad (2)$$

Herein, the application conditions are assumed as follow:

$$y = -2b, \quad x = \pm a; \quad y = 0, \quad x = a + 2b \tan \theta;$$

$$x = 0, \quad y = b_1; \quad y = -(b_2 + l)$$

that is:

$$l = \frac{\lambda b - a \tan \theta - b \tan^2 \theta}{\lambda} \quad (3)$$

$$b_2 = \sqrt{\frac{a^2 + \lambda(l - 2b)^2}{\lambda}}$$

Therefore, the height of the arch, namely b_2 , can be expressed by the following equation:

$$b_2 = \sqrt{\frac{(a + 2b \tan \theta)^2 + \lambda l^2}{\lambda}} \quad (4)$$

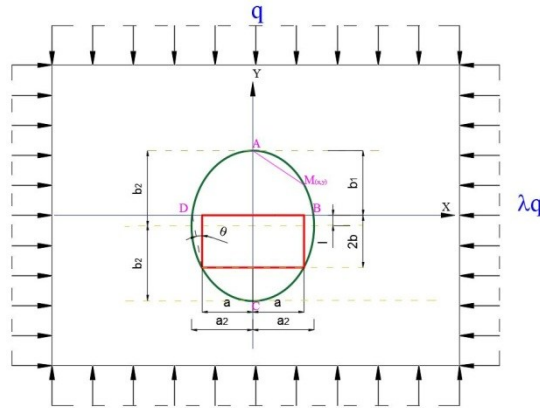


Figure 5. A sketch of the revised natural equilibrium arch [15].

3.2. Symmetric constraint condition with opposite boundary

According to the revised natural equilibrium arch theory, the load carried by the roof is calculated by the simplification that the compound roof is emerged into the combination in this section, as shown in Figure 6.

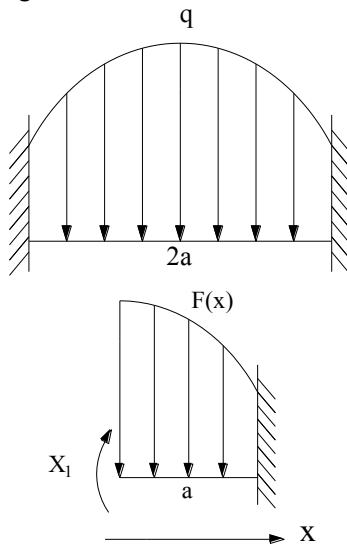


Figure 6. A simplified model for restricted roof.

Writing the equilibrium equation, we have:

$$F(x) = y = \sqrt{\frac{a_2^2 - x^2}{\lambda}} - l, \quad x \in (0, a) \quad (5)$$

$$\int M_p(x) dx = q \left\{ \frac{1}{2} \sqrt{\frac{1}{\lambda}} \left[\frac{x}{8} (2x^2 - a_2^2) \sqrt{a_2^2 - x^2} + \frac{a_2^4}{8} \arcsin \frac{x}{a_2} \right] + \frac{a_2^2}{2} \left[\left(\frac{x^2}{2} - \frac{a_2^2}{4} \right) \arcsin \frac{x}{a_2} + \frac{x}{4} \sqrt{a_2^2 - x^2} \right] \right. \\ \left. + \frac{1}{3} \sqrt{\frac{1}{\lambda}} \left[\frac{x}{8} (5a_2^2 - 2x^2) \sqrt{a_2^2 - x^2} + \frac{3}{8} a_2^4 \arcsin \frac{x}{a_2} \right] - \frac{1}{6} lx^3 - \frac{1}{3} \sqrt{\frac{1}{\lambda}} a_2^3 x \right\}$$

Taking the unit moment of X_1 , the moment curve and its corresponding M_p can be obtained as shown in Figure 7.

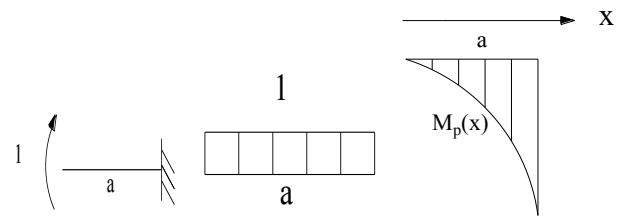


Figure 7. Moment corresponding M_p curves.

in which

$$\delta_{11} = \frac{1}{EI} (a \cdot 1) = \frac{a}{EI},$$

$$\Delta_{1P} = \frac{1}{EI} \left(\int_0^a M_p(x) dx \right) \cdot (-1) = -\frac{1}{EI} \int_0^a M_p(x) dx$$

When the angle at X_1 is equal to zero, we have:

$$\delta_{11} X_1 + \Delta_{1P} = 0$$

Then solving it yields:

$$X_1 = \frac{\int_0^a M_p(x) dx}{a} \quad (6)$$

in which:

3.2.1. Effect of additional supports

Figure 8 presents the situation where some additional standing supports are applied to strengthen the roof. Herein, t is the row space of each standing support.

Considering the symmetry of the load and boundary conditions, half of the model is presented herein for further discussion. Drawing the figure in terms of the unit moment of X1, for example, the moment curve obtained and its corresponding M1 can be seen in Figure 9.

Using a similar analysis for the unit of X2, we have the three graphs shown in Figure 10.

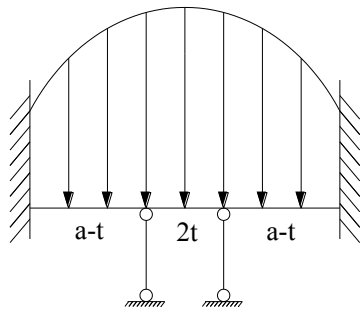


Figure 8. A simplified model for restricted roof with additional supports.

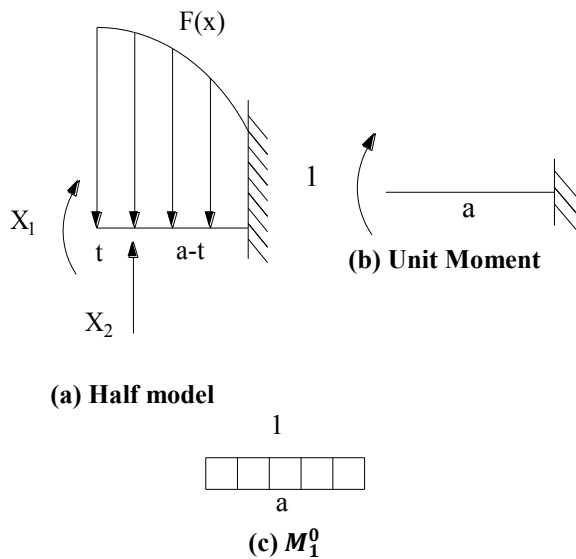


Figure 9. Analysis of unit element of X1.

$$A = \int_0^a M_p(x) dx, \quad B = \int_t^a (x-t)M_p(x) dx$$

$$\int xM_p(x) dx = q \left[\frac{a_2^2}{6} x^3 \arcsin \frac{x}{a_2} + \frac{1}{18} a_2^2 (x^2 + 2a_2^2) \sqrt{a_2^2 - x^2} - \frac{1}{30} \sqrt{\frac{1}{\lambda}} x^2 (a_2^2 - x^2)^{\frac{3}{2}} - \frac{2}{15} \sqrt{\frac{1}{\lambda}} a_2^2 (a_2^2 - x^2)^{\frac{3}{2}} - \frac{1}{8} t x^4 - \frac{1}{6} \sqrt{\frac{1}{\lambda}} a_2^3 x^2 \right]$$

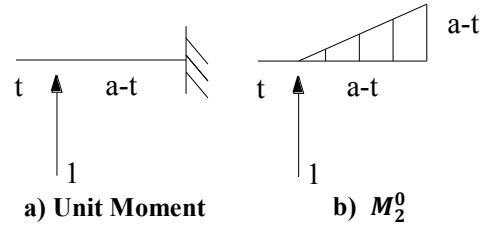


Figure 10. Analysis of unit element of X2.

Then it can be found that:

$$\delta_{11} = \frac{a}{EI},$$

$$\delta_{12} = \delta_{21} = \frac{(a-t)^2}{2EI},$$

$$\delta_{22} = \frac{1}{EI} \cdot \frac{1}{2} (a-t)^2 \cdot \frac{2}{3} (a-t) = \frac{(a-t)^3}{3EI}$$

$$\Delta_{1p} = -\frac{1}{EI} \int_0^a M_p(x) dx,$$

$$\Delta_{2p} = \frac{1}{EI} \int_t^a M_2^0(x) \cdot M_p(x) dx,$$

$$M_2^0(x) = x-t, \quad x \in (t, a)$$

Based on the restriction condition that the rotation at point X1 is zero and the vertical displacement at point X2 is equal to zero as well, the following equations can be obtained:

$$\begin{cases} \delta_{11}X_1 + \delta_{12}X_2 + \Delta_{1p} = 0 \\ \delta_{21}X_1 + \delta_{22}X_2 + \Delta_{2p} = 0 \end{cases} \quad (7)$$

$$\Rightarrow \begin{cases} a \cdot X_1 + \frac{(a-t)^2}{2} \cdot X_2 - A = 0 \\ \frac{(a-t)^2}{2} \cdot X_1 + \frac{(a-t)^3}{3} \cdot X_2 - B = 0 \end{cases}$$

Where:

Solving yields:

$$X_1 = \frac{4(a-t)A - 6B}{(a-t)(a+3t)} \tag{8}$$

$$X_2 = \frac{12aB - 6(a-t)^2 A}{(a-t)^3(a+3t)}$$

As discussed earlier, it is very important to change the distribution of the moment and reduce the deformation of the roof for the longwall installation roadway. Herein, the hydraulic support was selected as the standing support to evaluate the effect of the standing support. In fact, some other types of standing supports can also be used to play a similar role to control the stability of the roadway.

Different row spaces of hydraulic support ranging from 0.3 m to 0.7 m with a continuous increase of 0.1 m were applied and compared to explore the effect of the standing support. The calculated moment curves for different situations are presented in Figure 11.

It is apparent that the critical area has changed using the additional standing support as a secondary support, i.e. although the load on the top surface of the roof was still in compression, at the point of the 1/4 span, the tensile stress was also found on the top surface. In addition, the proper row space of the secondary support, namely the support density, is believed to be the critical parameter in practical design through comparison of the moment diagram.

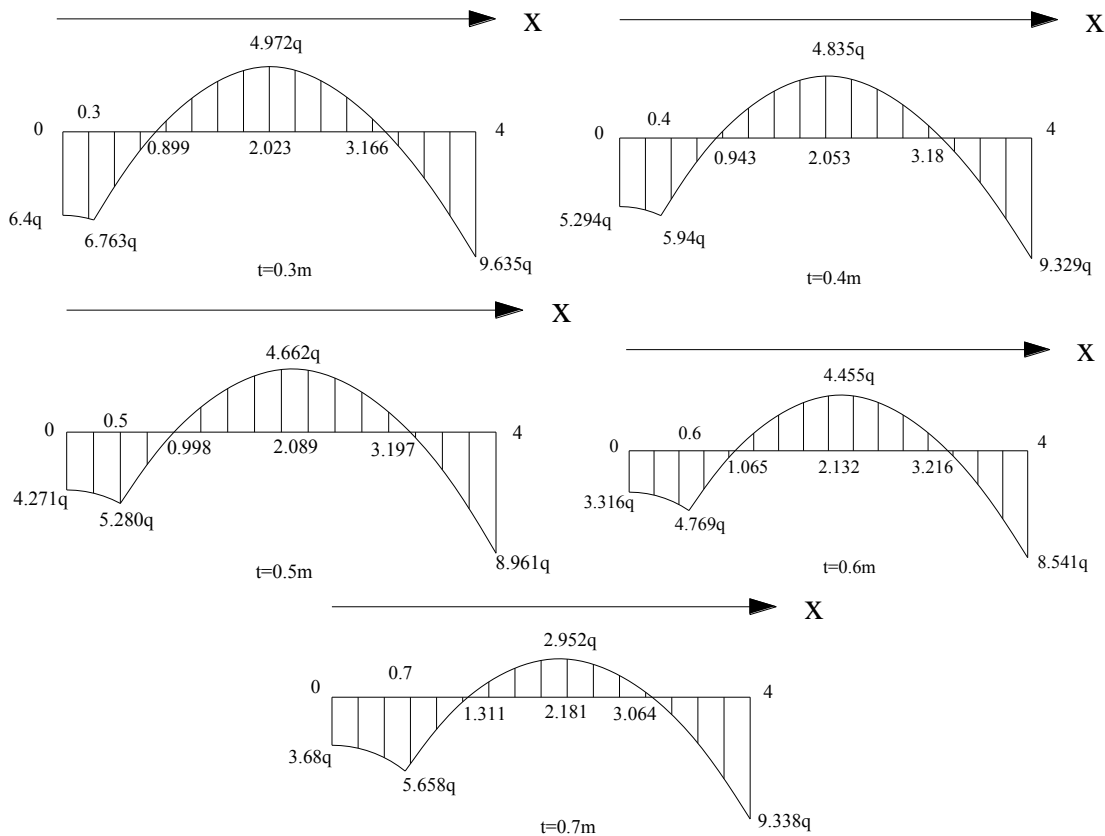


Figure 11. Moment diagram of roof with different spaces of standing support.

3.3.2. Effect of width of longwall installation roadway

In order to evaluate the effect of the width of the longwall installation roadway, two different widths of the longwall installation roadway (i.e. 4 m and 8 m) were adopted in the present research work. Herein, some key parameters referred to the geological condition are introduced as follow:

$$\lambda = 1, \quad b = 1.8m, \quad \varphi = 24^\circ \text{ and}$$

$$\theta = \frac{\pi}{4} - \frac{\varphi}{2} = 33^\circ$$

Figure 12 presents the moment diagram of these mentioned longwall installation roadways with different widths. Considering the symmetry of the load and boundary, only half of the moment curves are compared herein.

It is worth noting that the peak values of the moment normally occur at the middle and the boundary site of the roadway, as shown in Figure 12. As expected, it can also be found that the load on the roof is mainly in compression on the top surface. However, the tensile stress mainly exists on the bottom surface of the roof.

Compared to the roadway with a width of 4 m, the stress increases to about 7 times when the width increases to 8 m. In addition, it should be noted that an increase in the width not only leads to the increment of the stress but also changes the distribution of the moment. This situation is more serious for a roadway with compound roof, where the bonding strength of different strata is not

strong enough. Although it is difficult to maintain the stability of the surrounding rock, particularly for the roof, by enhancing the density of the primary support, a proper adjustment in terms of the span of roadway is regarded as one of the effective methods to change the distribution of moment. In other words, the roadway can be firstly caved and supported immediately with an acceptable width. Then the left part of the roadway is constructed to target width to reduce the nominal span of the roadway at the same time. The so-called “two-pass” that will be presented later in this paper is an example to reduce the nominal span by changing the caving procedure.

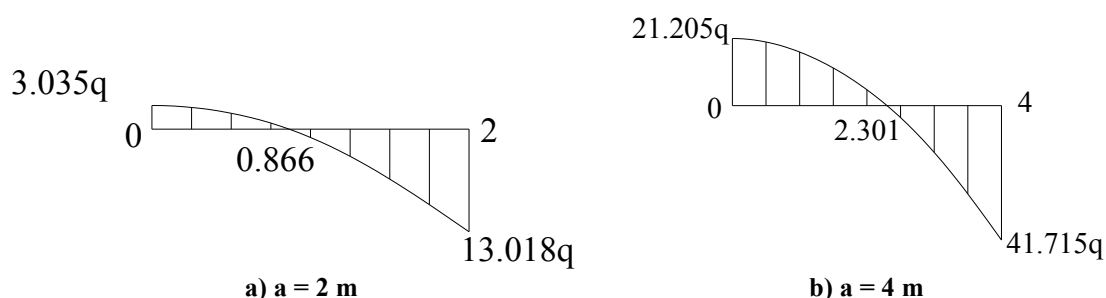


Figure 12. Moment diagram of roof with different spans of roadway.

4. Numerical modeling on longwall installation roadway under compound roof

4.1. Model setup

Numerical modeling was carried out for a further research work in terms of the caving method and critical parameters for support through the commercial finite analysis software program FLAC3D, version 3.0. The Mohr-Coulomb model was used to simulate the caving procedure of the longwall installation roadway with large cross-section under compound roof. The key parameters including the elastic modulus and friction angle of the surrounding rocks were calibrated based on an

experimental investigation in the laboratory. More detailed information about the simulation can be found in Table 1.

Considering the calculation capacity of the computer, the reduced cubic model with a width of 60 m was set up, as shown in Figure 13. Both sides of the model were fixed except for the top surface, which was free in the vertical direction to apply the vertical load on. The vertical load applied on the top surface is the sum of the gravity of overlying strata to simplify the calculation. The longwall installation roadway is located at the middle of the 3D model.

Table 1. Flac3D longwall installation roadway reconsolidation parameters.

Type of strata	UCS (MPa)	Tensile strength (MPa)	Elastic Modulus (GPa)	Shear Modulus (GPa)	Possion ratio	Cohesion (MPa)	Friction angle (°)	Density (kg·m ⁻³)
Mudstone	20.2	2.2	4.5	2.8	0.26	6.2	39.5	2400
Coal	10	1.2	1.5	1	0.30	2.8	25	1400
Fine sandstone	47	5.8	10.3	6.3	0.22	8.2	39.3	2600
9# coal	12	1.4	1.6	1.1	0.32	3.1	25	1400
Gray sandstone	29.4	3.1	9.7	6.1	0.25	7.3	40.1	2500
Silty mudstone	19.8	2	3.8	2.5	0.24	5.8	39.1	2400
Siltstone	21.6	1.8	5.1	2.7	0.25	5.2	27	2450
Limestone	50	5.6	21	11.5	0.30	11.5	41	2700

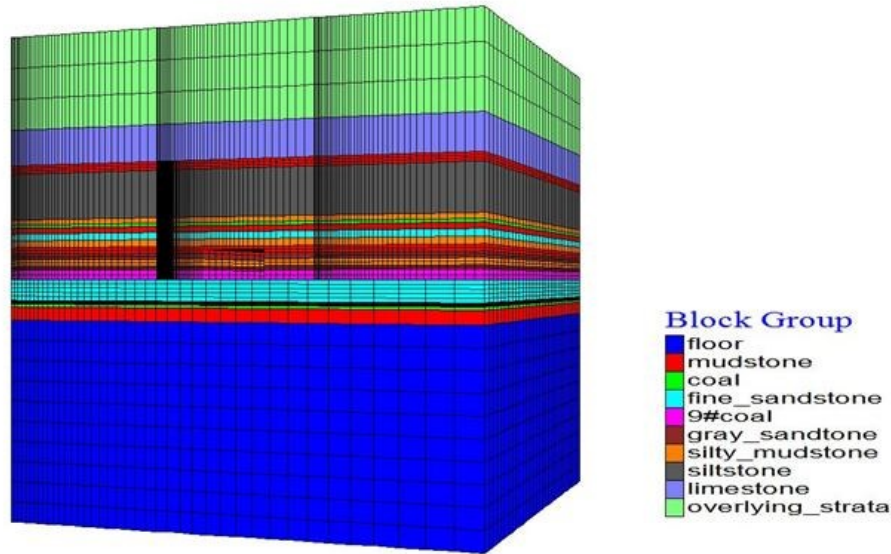


Figure 13. Flac3D model for simulation.

4.2. Effect of caving method

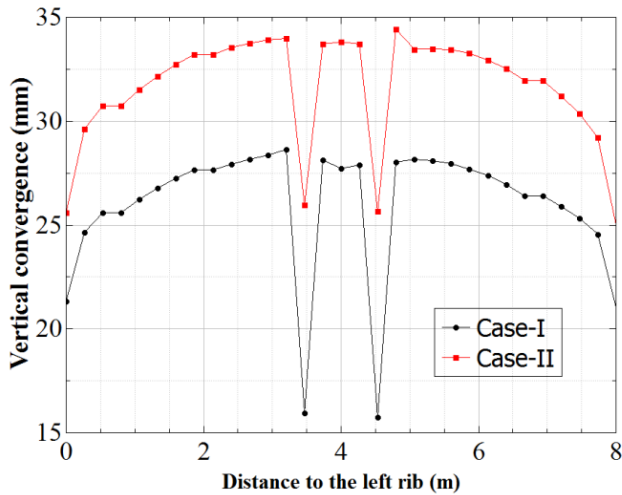
As discussed earlier, the caving method is the critical issue, which affects the stability of the longwall installation roadway with a large-scale cross-section. For a roadway with a normal size, one pass is usually adopted; however, with an increase in the width, the roadway should be constructed progressively, from once to several times according to either the size of the roadway or the geological condition.

Based on the complex geological condition of the longwall installation roadway discussed in the present paper, the “two-pass” caving method is believed to be an effective method to change the distribution of the stress on the compound roof that is sensitive to the span of roadway. Compared to its counterpart, the change in the caving method can successfully improve the stability of the surrounding rocks and postpone the separation of the overlying compound roof. Two different caving parameters were used for simulation to evaluate the effect of the caving method and demonstrate the expected advantages of the “two-pass” caving method. Herein, the initial caving widths (i.e. 4 m and 5 m) were compared and discussed, respectively. Correspondingly, two caving procedures termed as “4 m + 4 m” and “5 m + 3 m” were formed to maintain the designed width of the roadway (i.e. 8 m). In the present simulation, two rows of hydraulic props were applied nearby the central line of the roadway, and the space between each other was 1 m.

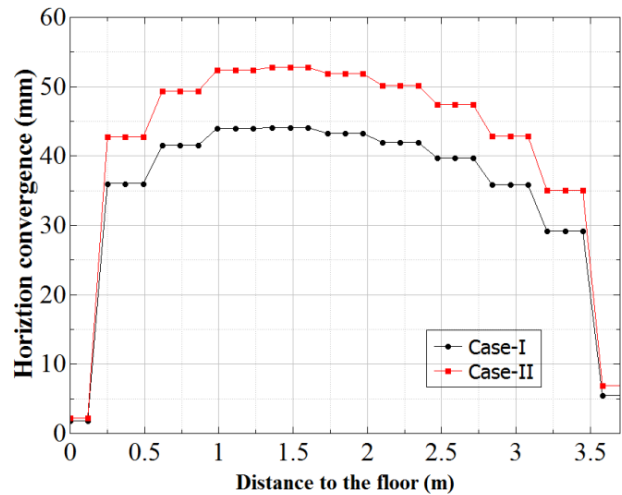
As shown in Figure 14, the convergence obtained from different caving methods is obvious. Compared to Case II, the overall deformation of the surrounding rocks using the caving procedure (i.e. “4 m + 4 m”) is relevantly smaller due to a decrease in the roadway span at the early stage. It is interesting to note that the vertical convergence experiencing a sharp decline nearby the central line (e.g. 4 m shown in Figure 14a) is attributed to the use of hydric prop in that area.

4.3. Effect of support density

In this section, the effect of the support density on the convergence of surrounding rock is discussed. As mentioned earlier, the additional support can significantly change the distribution of the moment on the natural equilibrium, resulting in a decrease in the deformation of the surrounding rocks. Figure 15 shows the comparison of the convergence for different support densities. The convergence obtained from the roadway without any support was compared with these with support as well. As expected, an increase in the support density leads to a decrease in convergence both in the vertical and the horizontal deformations. It should be noted that the installation of bolts and cables may play a similar effect to reduce the convergence of the surrounding rocks. However, the effect of hydraulic prop is only discussed herein to illustrate the possible method to improve the stability of the surrounding rocks.

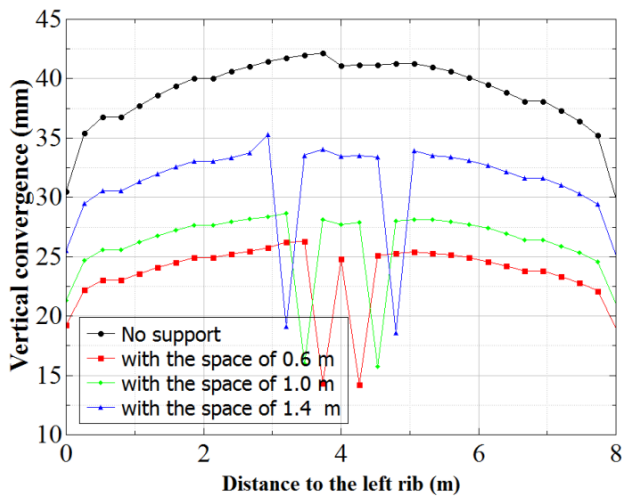


a) Vertical convergence

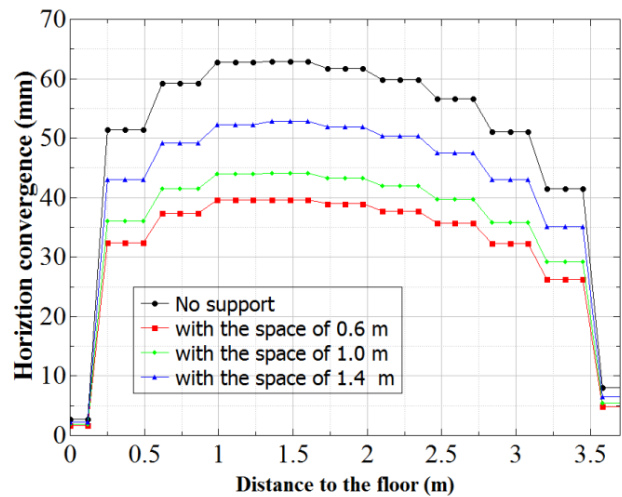


b) Horizontal convergence

Figure 14. Convergence obtained for different caving methods.



a) Vertical convergence



b) Horizontal convergence

Figure 15. Convergence obtained for different support densities.

5. Engineering application

Both the mathematical and numerical simulation analyses revealed that it was effective to maintain the stability of the surrounding rocks by reinforcing roof and/or changing the caving procedure. Based on the mentioned results, the engineering application conducted at the same installation roadway is presented hereafter.

The caving procedure with “two-pass” was adopted for the longwall installation roadway located at the No.90103 working panel presented earlier. As shown in Figure 16(a), the first pass started from the boundary to the working face with a distance of 4 m, and the reinforced support was immediately applied to the roadway to prevent the fracture evolution, as shown in Fig. 16(b). Compared to the convenient support shown in Figure 2, the obvious change in the proposed

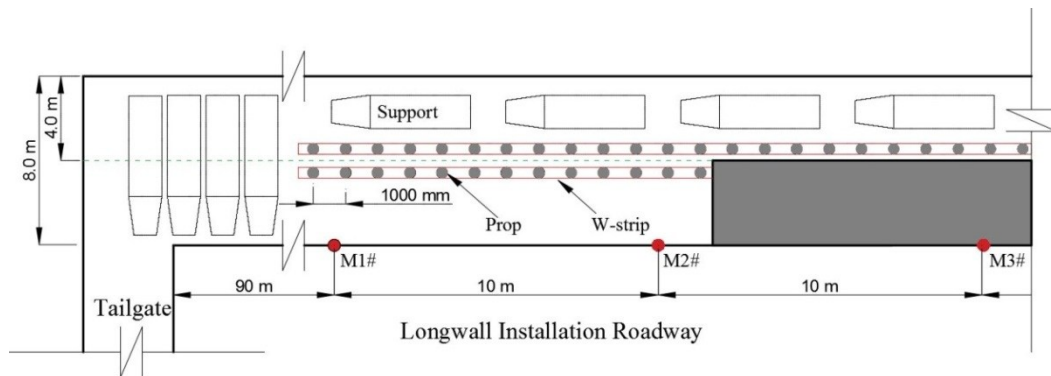
primary support (Figure 16) is the length of bolt increase from 1600 mm to 2400 mm. In addition, the hydric props topped with the W-shape steel strip were set up along the edge of the roadway with a width of 4 m. Moreover, the miners were well-trained to guarantee the quality of support installation to avoid the influence caused by the human factor. The field investigation indicated that the proposed support technology with the optimum parameter could maintain the roadway stability.

After caving of the first pass, the hydraulic support was transported and placed into the longwall installation roadway as reinforcement for the existing primary standing support. Three monitoring points were set up with a distance of 10 m apart from each other to investigate the deformation of the surrounding rocks. The first

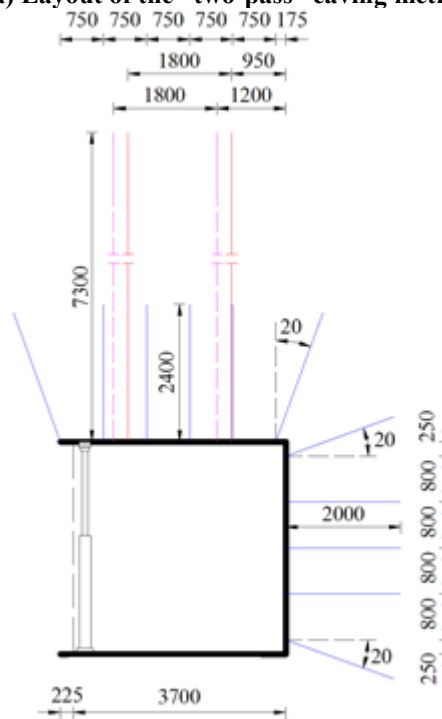
monitoring point termed as M1# was installed apart from the caving face with a distance of 90 m to avoid the influence caused by tailgate. Figure 17 shows the final support sketch with two-pass for the longwall installation roadway.

It is obvious that both the vertical and the horizontal convergences were kept at the acceptable level for normal use, as shown in Figure 18. Compared to the horizontal convergence, the relevant deformation occurring between the roof and floor was much larger than the simulation due to underestimation of the effects of bolts and cables. With caving the second pass of the longwall installation roadway, the increase in the deformation became stable, indicating that the applied support including the primary support and secondary support played their roles in controlling the movement of the surrounding rocks. In addition, the measured filed

data from different sites also demonstrated that it was very important to prevent the deformation of the surrounding rocks at an early stage. Compared to the simulation results, as shown in Figure 18, the values for the convergence obtained from the field test are generally smaller than those in the simulation, except for the vertical convergence measured at the first monitoring point (i.e. M1#). The reason for the smaller value of the field test is believed to be the underestimated consideration of the role played by the hydric support as a temporary standing support in the practical application. The scatter for vertical convergence obtained from different monitoring points is mainly due to the discordant deformation between the roof and floor, in particular for M1#, where the deformation is obviously different from the other two points.



a) Layout of the “two-pass” caving method



b) The support for the first “pass”

Figure 16. Sketch of the “two-pass” caving procedure.

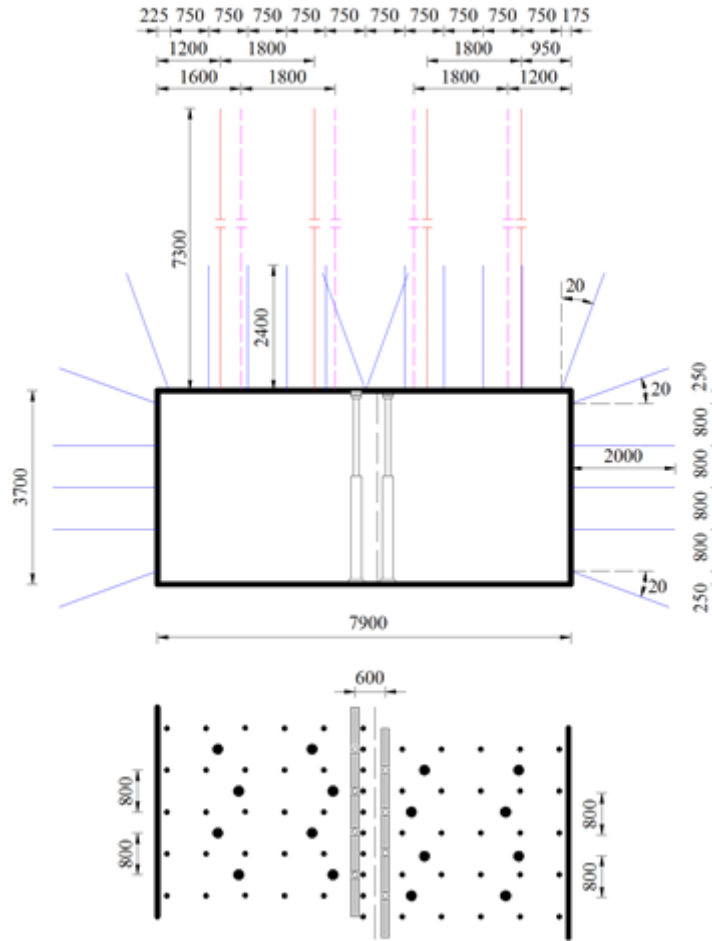
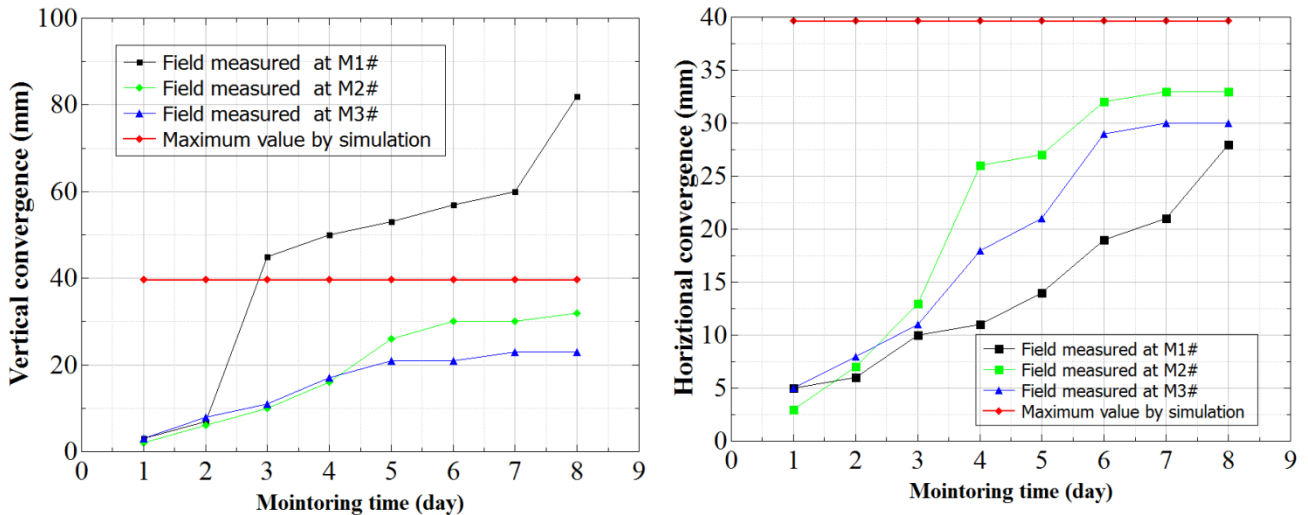


Figure 17. Cross-section of the longwall installation roadway with support.



a) Vertical convergence b) Horizontal convergence
 Figure 18. Deformation of surrounding rock obtained from field application.

6. Conclusions

In order to better understand the deformation characters and the failure mode of the large cross-sectional longwall installation roadway under compound roof, a theoretical analysis model with simplification was proposed to evaluate the effect

of the caving method as well as the support strength for the stability of the surrounding rocks. The finite analysis by FLAC3D was conducted to verify the conclusion obtained from a theoretical analysis. Based on the combined discussion, a case study with field investigation was carried out

to demonstrate the advantages of the proposed theoretical model as well as the optimum parameters. The results obtained from the present work can be summarized as follow:

1) The overlying strata nearby the surface of the roof is seriously affected by an increase in the cross-sectional size of the longwall installation roadway. Due to the lower tensile strength of the overlying strata, it is very important to strengthen the roof to prevent the de-bonding associated with the unexpected separation of different strata under compound roof condition.

2) Based on the revised natural equilibrium arch apsidal equation, the simplified theoretical analysis model presented in this work indicate that the reason for the failure of the overlying strata is mainly due to the occurrence of flex moment, which normally appears nearby the center line of the large cross-sectional roadway. This model that can also be used to evaluate other types of roadway with large cross-sections indicate that it is possible to maintain the stability of the surrounding rocks by changing the caving procedure to reduce the nominal width of the roadway.

3) The “two-pass” caving method verified by the successful case study of longwall installation roadway with acceptable deformation provides a reference to other types of roadway with similar geological conditions. Different from the conventional support technology, the use of hydric support as a temporary standing support combined with the traditional support technology is believed to be an effective method in practical applications.

Acknowledgments

The authors would like to express their thanks to the Research Fund of the State Key Laboratory of Coal Resources and safe Mining CUMT (SKLRSM18KF04) for the financial support of this work.

References

[1]. Jiang, L.S., Ma, N.J., Bai, L., Li, Y.J. and Zhang, L. (2014). Deformation and failure characteristics and roof caving hidden danger classification of roadways compound roof. *Journal of China Coal Society*. 39 (7): 1205-1211.

[2]. Manchao, H.E., Gan, Q.I. and Cheng, C. (2007). Deformation and damage mechanisms and coupling support design in deep coal roadway with compound roof. *Chinese Journal of Rock Mechanics and Engineering*. 26 (5): 987-993.

[3]. Xiao, T.Q., Bai, J.B., Wang, X.Y., Chen, Y. and Yu, Y. (2011). Stability principle and control of surrounding rock in deep coal roadway with large section and thick top-coal. *Rock and Soil Mechanics*. 32 (6): 1874-1880.

[4]. Chengwen, Z., Kun, L., Ruibin, H., Xiangyang, T. and Feiqi, W. (2016). Research on reasonable supporting parameters of roadway with complex roof. *China Coal*. 5: 014.

[5]. Zhang, Z., Xie, G., Wang, L. and Wang, H. (2017). Study on Surrounding Rock Deformation Failure Law and Soft Rock Roadway Support with Thick Composite Roof. *Journal of Engineering Science & Technology Review*. 10 (4).

[6]. Frith, R., Reed, G. and McKinnon, M. (2018). Fundamental principles of an effective reinforcing roof bolting strategy in horizontally layered roof strata and areas of potential improvement. *International Journal of Mining Science and Technology*. 28 (1): 67-77.

[7]. Colwell, M. and Frith, R. (2013). Analysis and design of faceroad roof support (ADFRS).

[8]. Seedsman, R. (2015). Preinstalled Cable Bolts in Longwall Installation Roads.

[9]. Bai, Q.S., Tu, S.H., Zhang, C. and Zhu, D. (2016). Discrete element modeling of progressive failure in a wide coal roadway from water-rich roofs. *International Journal of Coal Geology*. 167: 215-229.

[10]. Bai, Q.S. and Tu, S.H. (2016). Failure analysis of a large span longwall drift under water-rich roofs and its control techniques. *Engineering Failure Analysis*. 67: 15-32.

[11]. Payne, D.A. (2008). Crinum Mine, 15 Longwalls 40 Million Tonnes 45 Roof Falls-What did we Learn?.

[12]. Zakharov, V.N. and Malinnikova, O.N. (2018). Modeling geomechanical and geodynamic behavior of mining-altered rock mass with justifying mechanisms of initiation and growth of failure zones. In *Geomechanics and Geodynamics of Rock Masses, Volume 1: Proceedings of the 2018 European Rock Mechanics Symposium* (p. 167). CRC Press.

[13]. Yuan, L. (2015). Theory and practice of integrated coal production and gas extraction. *International Journal of Coal Science & Technology*. 2 (1): 3-11.

[14]. Razumov, E.A., Klishin, V.I., Opruk, G.Y. and Grechishkin, P.V. (2016). Rockbolting improvement in Coal Mines in permafrost regions. *Journal of Mining Science*. 52 (5): 949-955.

[15]. Miao, X. (1990). Natural equilibrium arch theory and the stability of roadway. *Journal of Mining & Safety Engineering*. 2: 3.

مکانیسم تغییر شکل و طراحی بهینه برای راهروهای نصب در روش جبهه کار طولانی با سقف مرکب

H.C. Zhao^{1 and 2*}, H.J. An³ and M.S. Gao^{1 and 3}

1- School of geology and mining engineering, Xinjiang University, Urumqi, Xinjiang, China

2- School of Civil, Mining and Environmental Engineering, University of Wollongong, Wollongong, NSW, Australia

3- School of Mines, China University of Mining and Technology, Xuzhou, Jiangsu, China

ارسال ۲۰۱۷/۱۰/۵، پذیرش ۲۰۱۸/۸/۶

* نویسنده مسئول مکاتبات: hz449@uowmail.edu.au

چکیده:

مشخصات تغییر شکل و حالت شکست راهروهای نصب جبهه کار طولانی تحت شرایط سقف مرکب به دلیل پیشرفت سریع تجهیزات مدرن معدنی، تبدیل به یک موضوع مهم شده است. برنامه‌های کاربردی مختلف مهندسی نشان داده‌اند که طراحی و تکنولوژی نگهداری نامناسب از دلایل اصلی مرگ‌ومیرهای ناشی از حوادث سقوط ناگهانی سقف ناشی از جدایش لایه‌های سقف است. در پژوهش حاضر، با انجام مطالعه موردی استفاده از فناوری نگهداری سنتی به منظور نشان دادن اهمیت موضوع و خلاصه‌ای از حالات شکست در این راهروها با ضخامت‌های مختلف لایه‌ها مورد بحث و بررسی قرار گرفته است. سپس یک مدل تئوری ساده ارائه شده است و به منظور درک بهتر توزیع مناطق الاستیک- پلاستیک به عنوان تأثیرات روش‌های مختلف حفاری مورد بررسی قرار گرفته است. همچنین با استفاده از نرم‌افزار FLAC3D تأثیر روش حفاری و تقویت‌های انجام شده توسط سیستم‌های نگهداری اضافی مورد ارزیابی واقع شده‌اند. در مرحله بعد، یک مطالعه موردی در یک معدن زغال‌سنگ با شرایط سقف مرکب به منظور بررسی مزایای این روش طراحی ارائه شده، انجام شد. نتایج به دست آمده نشان می‌دهد که روش طراحی بهینه‌سازی شده ارائه شده در این پژوهش، برای کنترل تغییر شکل سنگ‌های اطراف، به خصوص در شرایط جدایش لایه‌های مرکب مؤثر است.

کلمات کلیدی: جبهه کار طولانی، راهروی نصب، سقف مرکب، مقطع عرضی بزرگ، تجزیه و تحلیل تئوری.
